Electronic Supplementary Material (ESI) for Journal of Materials Chemistry B.

Tumor Acidity/Redox Hierarchical-Activable Nanoparticles for Precise Combination of X-ray-Induced Photodynamic Therapy and Hypoxia-Activated Chemotherapy

Beibei Zhang[†, ‡], Rui Xue[†, ‡], Jisheng Lyu[†, ‡], An Gao[†], Chun-Yang Sun[†,*]

[†] Department of Radiology and Tianjin Key Laboratory of Functional Imaging, Tianjin Medical University General Hospital, Tianjin 300052, P.R. China

E-mail: chysunshine@gmail.com (C. Y. Sun)

MATERIALS AND METHOD

Materials and characterizations.

Disodium telluride and di(1-hydroxylundecyl) ditelluride were prepared according to the previous report.[1] Maleimide-terminated PEG (Mal-PEG$_{77}$-OH, Mn=3400) were purchased from Shanghai ToYongBio Tech. Inc. (Shanghai, China). Triethylamine, succinic anhydride and 2,3- dimethylmaleic anhydride were purchased from Alfa Aesar (Shanghai, China). $CHCl_3$ was refluxed over CaH_2 alloy under N_2 atmosphere and distilled just before use. 3-(4,5-dimethylthiazol-2-yl)-2,5-diphenyl tetrazolium bromide (MTT) was purchased from Sigma-Aldrich Chemical Co., Ltd.. Dulbecco's modified Eagle's medium (DMEM) and fetal bovine serum (FBS) were purchased from Life Technologies Corporation (Gibco, USA). All other reagents and solvents without statement were of analytical grade and used as received.

The proton nuclear magnetic resonance (^{1}H NMR) spectra were recorded in deuterated chloroform ($CDCl_3$) or deuterated dimethyl sulfoxide (DMSO-d_6) on a 400 MHz spectrometer (Avance III, Bruker, Germany). The size and zeta potential measurements were carried out in aqueous solution using a Malvern ZS90 dynamic light scattering instrument with a He-Ne laser (633 nm) and 90° collecting optics. The data were analyzed using Malvern Dispersion Technology Software 5.10.

ROS Generation *in Vitro*.

$^1O_2$ generation of VP-loaded nanoparticles was measured by singlet oxygen green sensor (SOSG) based on the reference.[2] 200 μL of free VP, ^{DA}TAT-NP$_{VT}$, ^{SA}TAT-NP$_{VT}$ or TAT-NP$_{VT}$ was mixed with SOSG (final concentration is 5 μM),

respectively. Following the X-ray radiation, the SOSG emission fluorescence at 525 nm were recorded by H-7000 fluorescence spectrophotometer (Hitachi, Japan, E_x = 488 nm) to reflect $^1O_2$ production.

TPZ Release *in Vitro* under different GSH Conditions.

To measure the TPZ release, ^{DA}TAT-NP$_{VT}$, ^{SA}TAT-NP$_{VT}$ or TAT-NP$_{VT}$ was suspended in phosphate buffer (PB, 20 mM, pH 7.4) with or without 10 mM of GSH. The solution was then transferred into the dialysis tubing (MWCO 14000 Da), which was incubated at 37 °C with gentle shaking (60 rpm). At predetermined intervals, the external PB buffer was collected and replaced by the fresh buffer. The TPZ content in collected PB was analyzed by high performance liquid chromatography (HPLC).

Cytotoxicity of TAT-NP, ^{DA}TAT-NP and ^{SA}TAT-NP.

MDA-MB-231 cells seeded in 96-well plate at 5000 cells per well, and incubated with TAT-NP, ^{DA}TAT-NP or ^{SA}TAT-NP pretreated at different pH conditions. The cell viabilities were measured by a standard MTT assay after further incubation of 72 h using a Bio-Rad 680 microplate reader.

Cytotoxicity by Live/Dead Cells Staining.

For live/dead cell staining, MDA-MB-231 cells were seeded in the 12-well plates at 40000 cells per well and incubated with TAT-NP$_{VT}$, ^{DA}TAT-NP$_{VT}$ or ^{SA}TAT-NP$_{VT}$ for 12 h. After washing twice with PBS and the replacement of fresh DMEM medium, cells were exposed to X-Ray irradiation (4 Gy) for 10 min. Then, the cells were further incubated at 37 °C for another 36 h, stained using a Calcein-AM/PI kit (Beyotime Biotechnology) following the manufacture's procedure.

Statistical analysis

The statistical significance of treatment outcomes was assessed using Student's *t*-test (two-tailed); $p < 0.05$ was considered statistically significant in all analyses (95% confidence level).

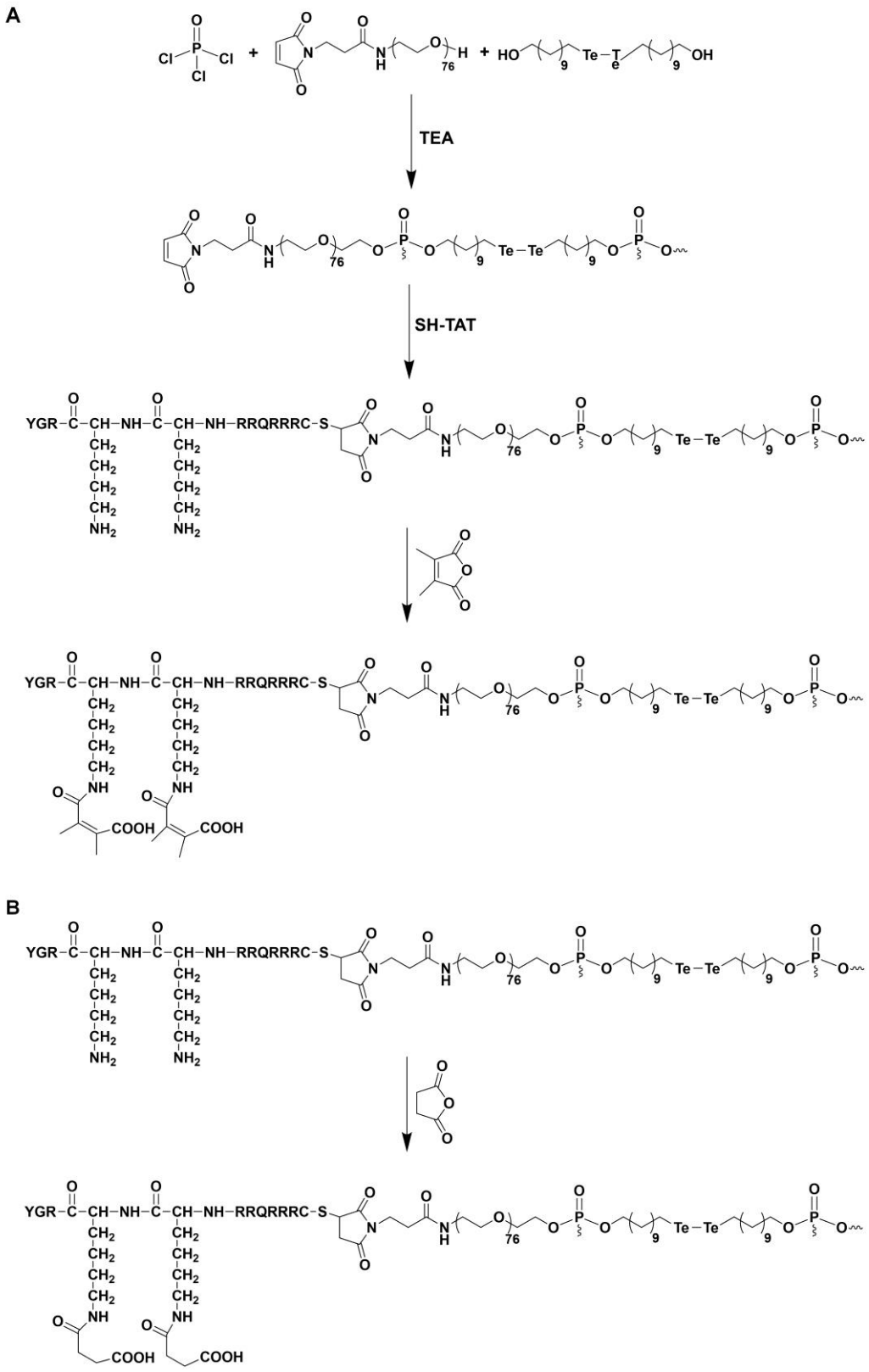

Figure S1. Synthetic route of DA (A) or SA (B) modified TAT-HPE.

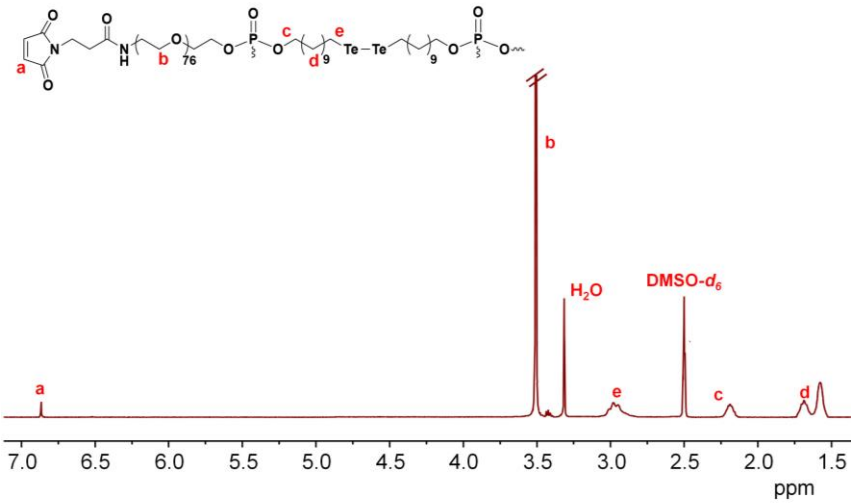

Figure S2. ^{1}H NMR spectrum of Mal-HPE in DMSO-d_6 recorded on an AVANCE III 400 MHz spectrometer at 25 °C.

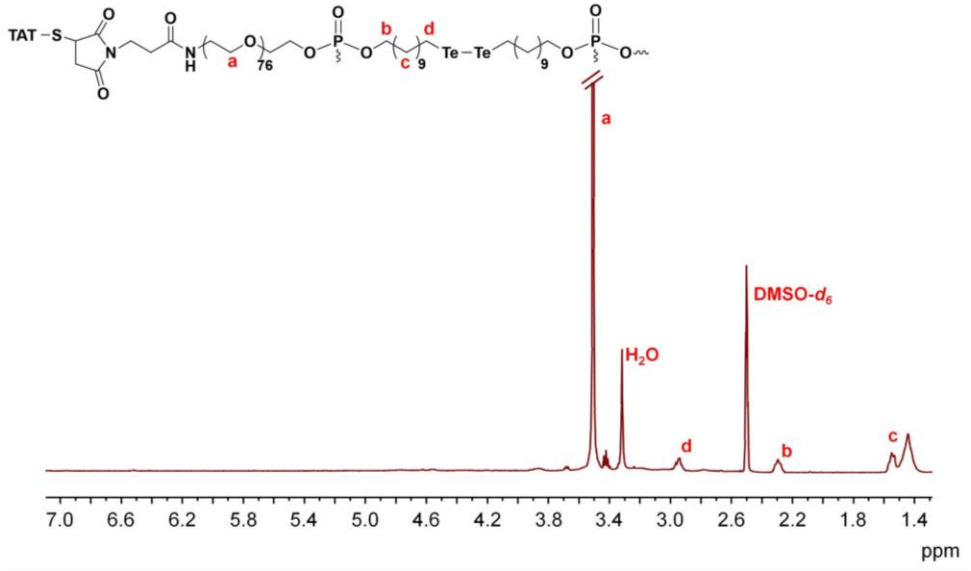

Figure S3. ^{1}H NMR spectrum of TAT-HPE in DMSO-d_6 recorded on an AVANCE III 400 MHz spectrometer at 25 °C.

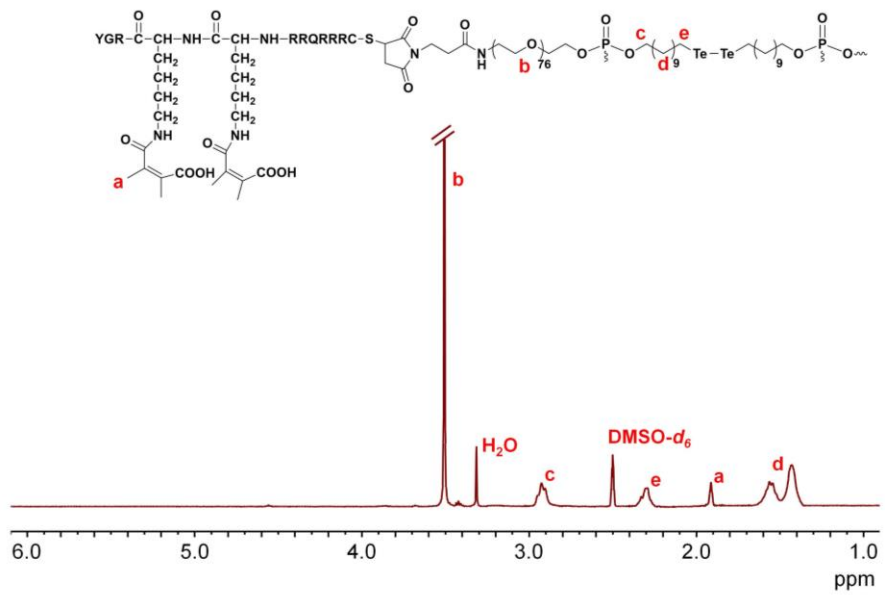

Figure S4. ^{1}H NMR spectrum of DA-modified TAT-HPE in DMSO-d_6 recorded on an AVANCE III 400 MHz spectrometer at 25 °C.

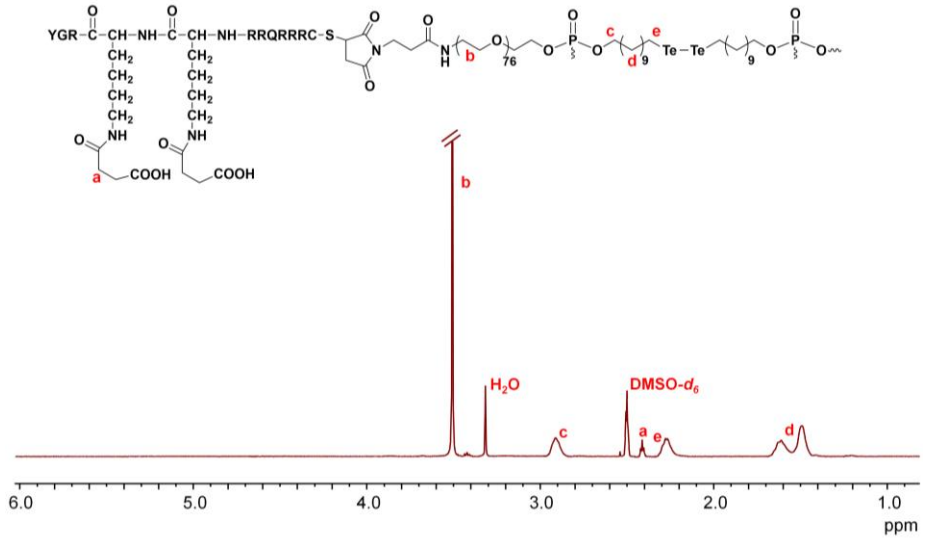

Figure S5. ^{1}H NMR spectrum of SA-modified TAT-HPE in DMSO-d_6 recorded on an AVANCE III 400 MHz spectrometer at 25 °C.

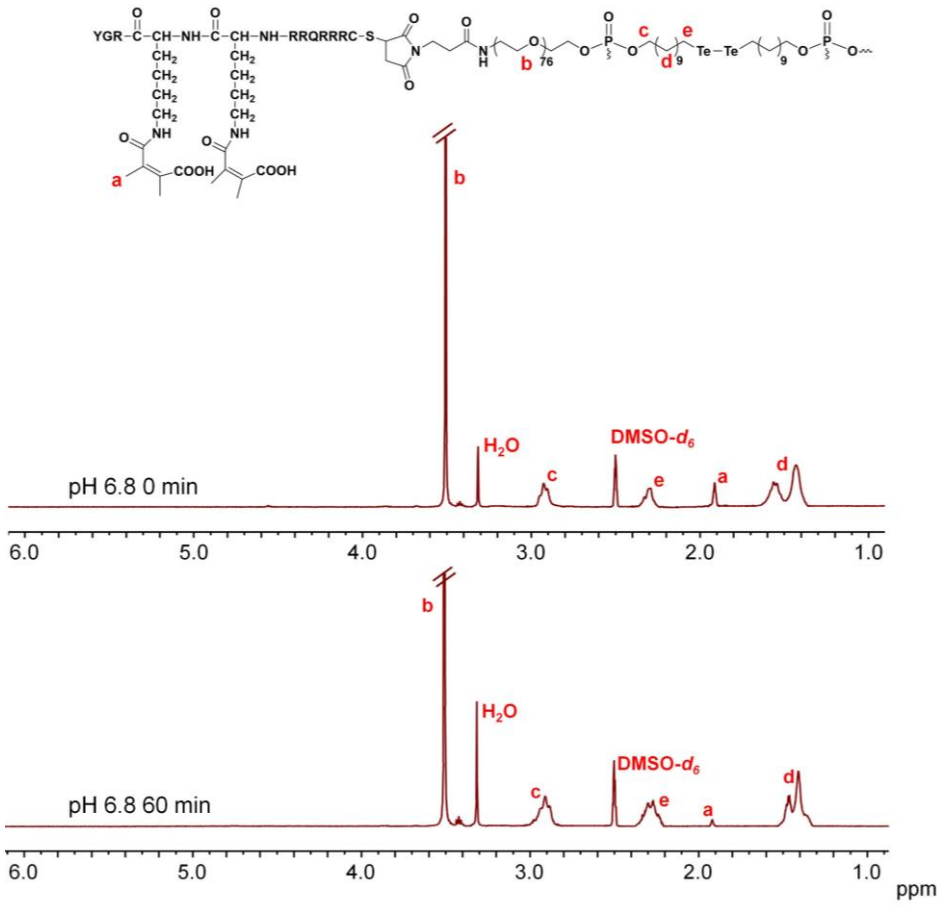

Figure S6. ^{1}H NMR spectrum of the ^{DA}TAT-NP after treatment at pH 6.8 for 60 min.

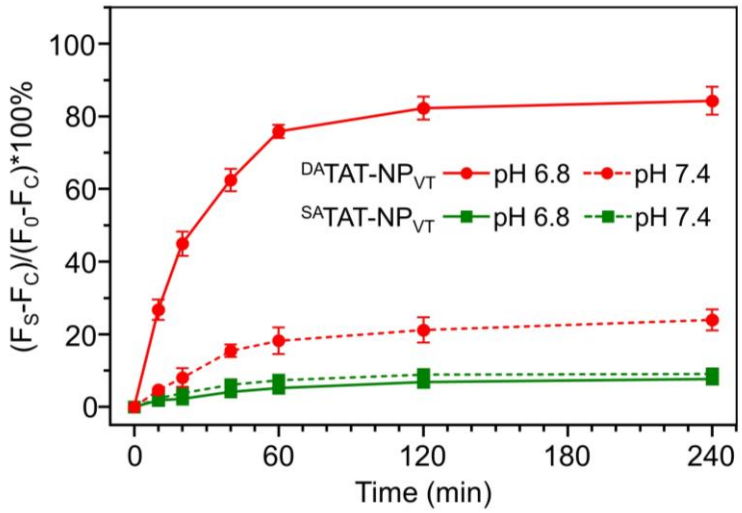

Figure S7. The degradation of ^{SA}TAT-NP$_{VT}$ and ^{DA}TAT-NP$_{VT}$ at pH 7.4 and pH 6.8. Fluorescamine was used as the sensor.

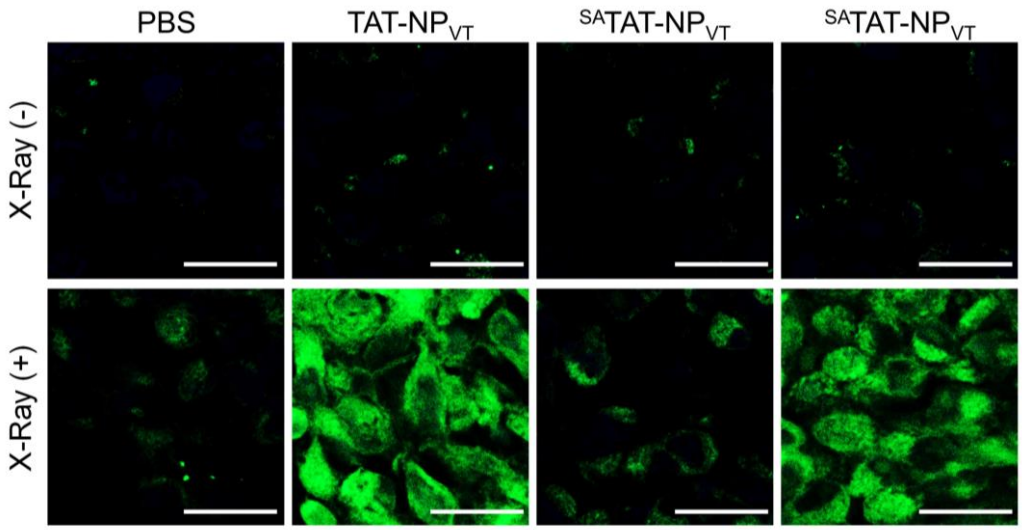

Figure S8. Hypoxia of MDA-MB-231 cells treated with PBS, TAT-NP_{VT}, ^{SA}TAT-NP_{VT} or ^{DA}TAT-NP_{VT} at pH 6.8 with or without X-ray irradiation. The scale bar is 20 μm.

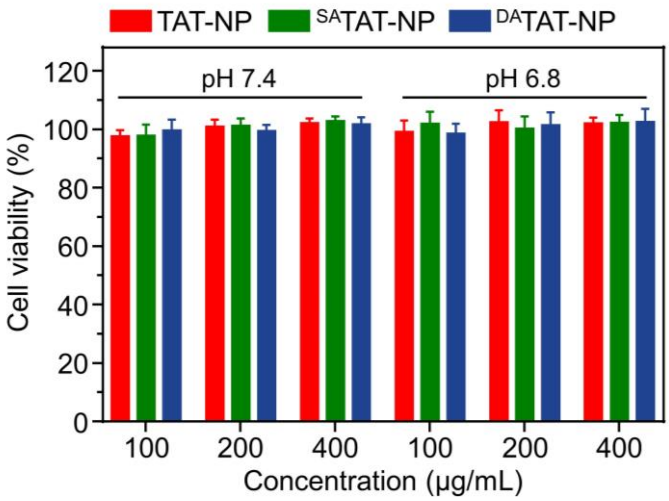

Figure S9. Relative cell viabilities after incubation with TAT-NP, ^{SA}TAT-NP or ^{DA}TAT-NP at pH 7.4 or 6.8.

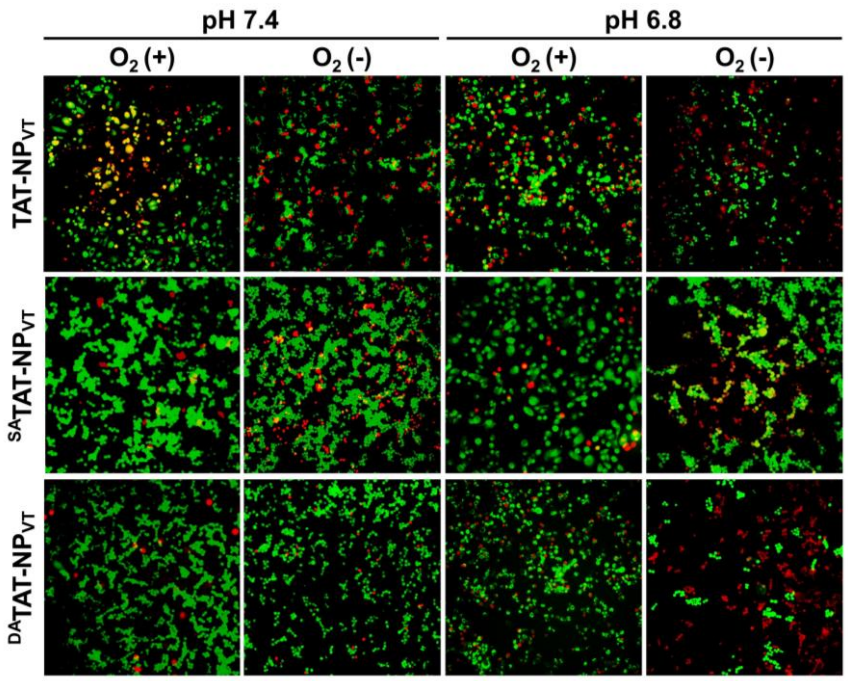

Figure S10. Live/dead staining of MDA-MB-231 cells after incubation with TAT-NP_{Ce6}, ^{SA}TAT-NP_{Ce6} or ^{DA}TAT-NP_{Ce6} at pH 7.4 or 6.8.

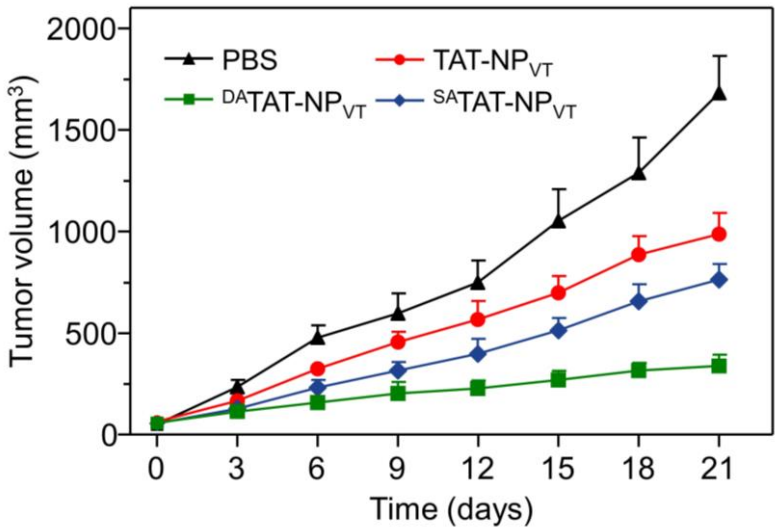

Figure S11. Tumor growth on mice bearing MDA-MB-231 tumor xenograft with different treatments (n = 5). The mice were received the irradiation of 4.0 Gy X-ray with the pork tissues of 1.0 cm thickness lain on top.

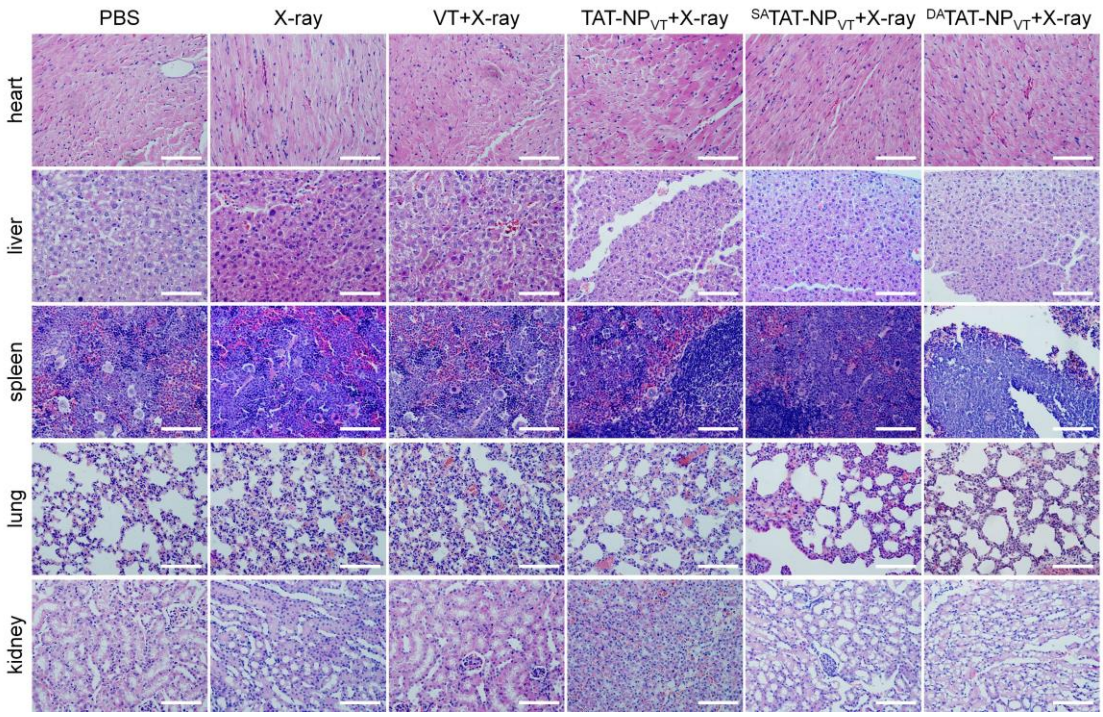

Figure S12. Histopathology analyses of visceral organ sections from MDA-MB-231 xenografted female mice after the tumor growth inhibition experiment. The scale bar is 200 μm.

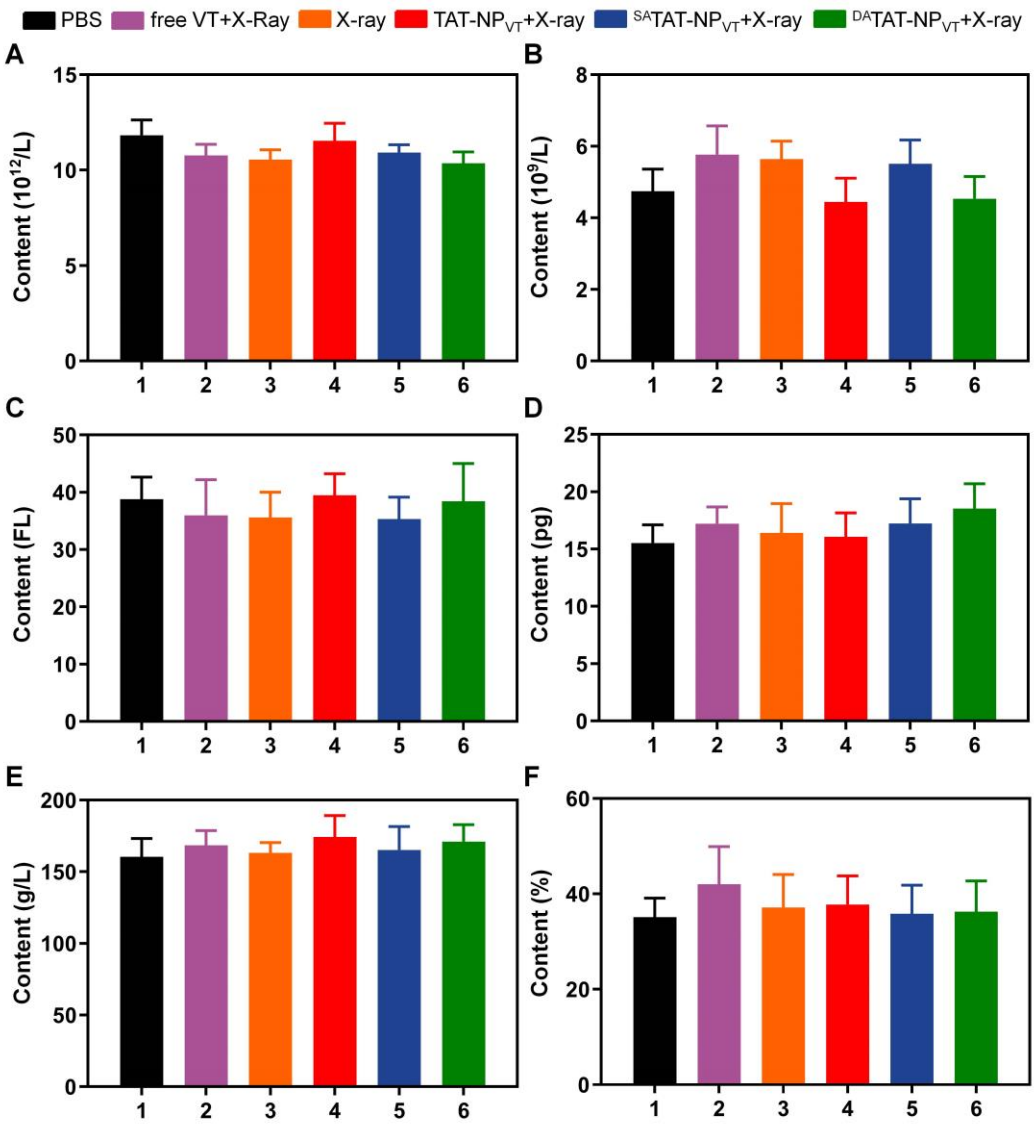

Figure S13. Hematology analysis of the mice after different treatments: (A) red blood cell (RBC), (B) white blood cell (WBC), (C) mean corpuscular volume (MCV), (D) mean corpuscular hemoglobin (MCH), (E) hemoglobin (HGB), and (F) hematocrit (HCT), respectively.

Table S1. Drug loading contents (DLC) and encapsulation efficiencies (EE) of TAT-NP_{VT}, ^{SA}TAT-NP_{VT} and ^{DA}TAT-NP_{VT}.

	DLC (%)		EE (%)	
	VP	TPZ	VP	TPZ
TAT-NP_{VT}	3.83±0.29	2.80±0.20	40.90±3.34	26.67±3.71
^{SA}TAT-NP_{VT}	4.06±0.43	2.60±0.22	43.47±4.72	27.83±2.30
^{DA}TAT-NP_{VT}	4.09±0.54	2.67±0.41	43.93±6.17	28.70±4.67

References

1. Y. Wang, L. Zhu, Y. Wang, L. Li, Y. Lu, L. Shen and L. W. Zhang, Ultrasensitive GSH-responsive ditelluride-containing poly(ether-urethane) nanoparticles for controlled drug release, *ACS Applied Materials & Interfaces*, 2016, **8**, 35106-35113.
2. W. Deng, K. J. McKelvey, A. Guller, A. Fayzullin, J. M. Campbell, S. Clement, A. Habibalahi, Z. Wargocka, L. Liang, C. Shen, V. M. Howell, A. F. Engel and E. M. Goldys, Application of mitochondrially targeted nanoconstructs to neoadjuvant X-ray-induced photodynamic therapy for rectal cancer, *ACS Central Science*, 2020, **6**, 715-726.